Journal of Robotics and Control (JRC)
Volume 3, Issue 5, September 2022
ISSN: 2715-5072, DOI: 10.18196/jrc.v3i5.15071

Optimization of Humanoid Robot Leg Movement Using Open CM 9.04

Agusma Wajiansyah [1], Rheo Malani [2], Supriadi [3], Achmad Fanany Onnilita Gaffar [4]
[1, 2, 3, 4,] Applied Modern Computing and Robotics System Unit, Politeknik Negeri Samarinda, Indonesia
Email: [1] agusma.wajiansyah@gmail.com, [2*] anaogie@gmail.com, [3] supriadi.polnes@gmail.com, [4] onnygaffar212@gmail.com
*Corresponding Author

Abstract— **The Indonesian Robot Dance Contest (KRSTI) is a branch of the Indonesian Robot Contest (KRI) with the theme of dance. The robot used is a humanoid robot that can dance. Every year at the event, the provisions for robots constantly change, both the type of dance being demonstrated and the requirements for the robot's height. The taller the robot, the more difficult it is to control its walking movements because of the load it carries. This study uses a suitable algorithm to make the walking movement more natural and minimize the robot's falling. Human ROM data is used as a parameter for the range of motion of the servos that act as joints in the robot's legs. The algorithm created serves to determine the initial position of the angle on the servo to avoid the wrong initial movement position between one servo and another. The robot used is the Bioloid Robot's leg Type A and uses OpenCM 9.04-A as the controller. The results showed that ROM on human feet could not be fully implemented on robot legs due to the robot's structure and the need for a robot that only relies on an algorithm to find the correct fulcrum to maintain balance. The comparison results show that the movement when walking on the ankle (ID servo 15) ranges from 749-567, while the ROM range is only between 580-512. When walking (servo ID 16), movement ranges from 460-291, while the ROM range ranges from 580-512.**

Keywords—Humanoid, ROM, Bioloid Type-A, OpenCM 9.04

I. INTRODUCTION

The Indonesian Dance Robot Contest (KRSTI) is a competition for the design, manufacture, and programming of robots accompanied by Indonesian art and culture elements, especially the art of dance known in the country. KRSTI is a branch of the Indonesian Robot Contest (KRI) with the theme of dance. This competition is held to increase student creativity and interest, especially in robotics technology which various universities are following. This competition branch is also intended to introduce the dance culture of an area used as the competition theme. The competition arena is divided into three zones, where every time the participant moves to the zone, the participants will get additional points besides the beauty points in dancing. For this reason, in this competition, the walking movement is considered essential [1].

Humanoid robots are robots that have human-like characteristics that were created to lighten the human burden. Along with the times, technology in humanoid robots is increasingly developing. Most of the existing technology is human implementation, starting from physical structure to intelligence. In the robot walking movement, the legs are a precarious part. As in the KRSTI competition, with the robot's height, equipment such as controllers and batteries and the accessories worn move the robot's legs have to withstand the existing load.

The impact of the robotics revolution has extended to human society. In this case, it should have had as significant an impact as the advent of the personal computer. At this time, it was widely accepted that personal robots would be anthropomorphic in shape, leading to increased interest in humanoid robotics. The shape and movement of the robot are related to its mechanical construction and actuators. The term anthropomorphic (commonly called humanoid) is usually associated with the outward appearance of a robot, with two legs, two arms, and head. The reason for choosing this form is because such a personal robot will maneuver best in the human environment, and humans will easily accept its human-like movements [2-5].

Designing a walking motion for a humanoid robot is a complex challenge. Many researchers have defined the walking motion using various approaches, one of which is the Linear Inverted Pendulum model [6-10]. Although this model is efficient for obtaining walking motion, the resulting gait is not very human-like. Moreover, the dynamic influence of various humanoid robot bodies is not taken into account.

The studies that have been carried out at [11-14] have outlined the main characteristics of human walking as follows: duration of different phases, step placement, CoM (Center of Mass) Trajectory, ZMP (Zero Movement Point) trajectory, swing foot motion, trunk motion, hip motion, and arm swing. The main characteristics of human walking are then used as the selected parameters to build a humanoid robot algorithm to walk like a human.

Several approaches to mimicking human movements have been developed, taking into account the various parameters associated with the human-like gait movement. Research on robot walking has been done a lot, which conditions the robot to walk like a human [2-5, 15, 16]. In the process of implementing the human-to-robot walking movement, the most important thing is the algorithm. A right algorithm needs to be made to imitate the way humans walk based adequately on specific parameters.

The right algorithm is the primary key added with the additional parameters that are there. Any parameter that is applied has the same goal of maintaining balance or minimizing so that the robot does not fall. Unlike humans who can adjust the balance by themselves, robots need the right algorithm design to maintain the balance. This study aims to optimize the movement of the robot's foot by implementing human foot motions in the robot to build a walking motion algorithm. The range of motion of the human foot/joint is used as a parameter of the joint movement of the robot's leg. The part studied was only the bioloid's leg robot type-A using OpenCM 9.04-A as a controller.

II. MATERIALS AND METHODS

A. Materials (Related Works)

Humanoid robots have that physical structure that resembles a human being, in whole or in part, namely, the limbs, torso, and head or, for example, from the waist up or down. Even some of them have equipped with faces, eyes, and mouths, just like humans. The hallmark of a complete humanoid is the upright pose combined with bipedal ambulation. Most mobile robots that rely on wheels, tracks, or other propulsion devices and mimic human ambulation have traditionally proved problematic. Likewise, achieving fall recovery and other instinctive human maneuvers has posed significant technological challenges. The main reason for the development of humanoid robots is to create a built environment around humans and are designed to operate to assist daily human activities. Likewise, they need to imitate human physical attributes such as size and dexterity if they are to operate tools, machines, vehicles, etc [5, 12, 15].

The main characteristics of a human walking as the selected parameters to build a humanoid robot algorithm to walk like a human are summarized as follows.

1. Duration of different phases

Human walking is based on significant events that occur during walking, which form a cycle of gait. The duration of the different phases is measured as a percentage of the cycle duration [14, 17-19]. A gait cycle consists of two steps: double support (DS) and simple support (SS), as shown in Fig. 1.

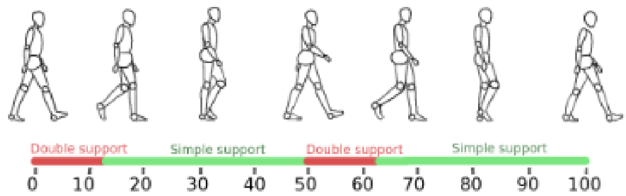

Fig. 1. SS and DS phases duration

2. Step placement

The step placement is related to the length and width of the step, which varies greatly depending on the morphology and age [14, 19-21]. Step placement is implemented on the humanoid robot using a series of footprints modeled in a certain way, as shown in Fig. 2[14, 22, 23].

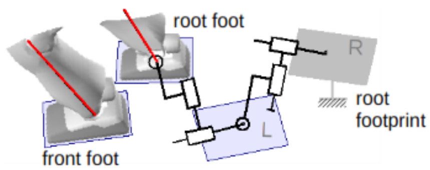

Fig. 2. The humanoid robot's articulated model to a series of footprints

3. CoM (Center of Mass) trajectory

The Human CoM trajectory is similar to a sine curve in the longitudinal, transverse, and vertical directions. In the transverse direction, the magnitude and period of the oscillations vary with velocity. In the vertical direction, the oscillation magnitude increases with speed and is equal to about 2% of the body height [24]. Various methods have been proposed for control humanoid robots that focus on the CoM trajectory generation, such as the Predictive Control (MPC) Model [25, 26], the minimized falling damage method which divided into two phases: (a). the optimal parametric strategy based on an inverted pendulum with flywheel used to plan the robot's motion, (b). the heuristic strategy to prevent the robot from bouncing and rolling over [27], and self-disturbance rejection control [28, 29]. An example of CoM trajectory generation based on predictive control is shown in Fig. 3 [6, 24, 30, 31].

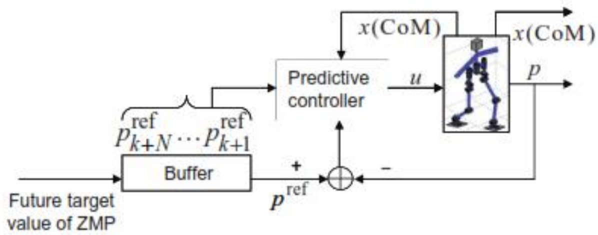

Fig. 3. CoM trajectory generation based on predictive control

4. ZMP (Zero Moment Point) trajectory

ZMP calculated from heel to toe corresponds to the rolling motion of the foot and mobility of the sole of the human foot. The trajectory of the ZMP changes depending on human footwear [8, 32, 33]. The concept of zero moment point (ZMP) is usually used to produce the horizontal trajectory of a humanoid robot. ZMP is an index to determine the stability of the robot. If the robot model is simplified, the ZMP equation also becomes very simple. Vice versa. By solving this equation analytically, the CoM trajectory with the ZMP of interest can be calculated quickly. One of the control methods applied is linear-quadratic optimal control to find the COM path that tracks the ZMP reference and is often used to create a walking trajectory for humanoid robots [8, 10, 26, 32, 34, 35].

5. Swing foot motion

The swing foot motion [36-38] consists of two components: the overall trajectory of the swing foot and the foot's orientation.

6. Trunk motion

The trunk [39, 40], which represents 60% by weight, has a significant angular oscillation. In the frontal plane, the oscillation amplitude varies from 3^o to 6^o. The basic idea of trunk-controlled motion is as follows: A balanced movement must always support the center of mass. In order to achieve this, the motion must be defined concerning the frame of reference with the center of mass as the origin. In addition, supporting the center of mass usually means acting against gravity, regardless of the actual tilt of the robot. Therefore, the orientation of the frame of reference must always be pointing upwards but still facing the horizontal view of the robot. More details are shown in Fig. 4.

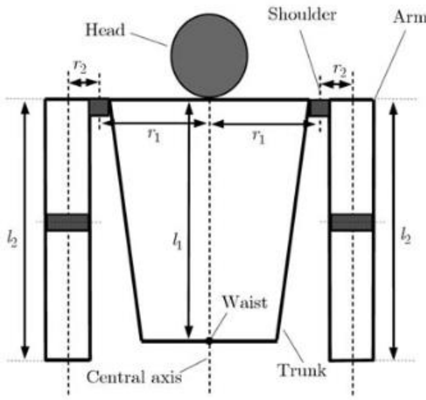

(a). the upper body

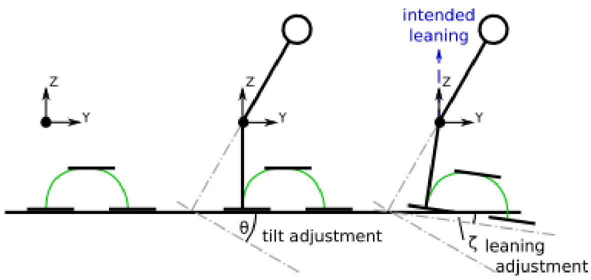

(b). An automatically adapted motion defined in the virtual motion frame

Fig. 4. Trunk controlled motion framework

7. *Hip motion*

The human body is a structure joined based on the structure and characteristics of the bone-muscle tissue. It reduces the response to muscle contraction and the body's energy consumption. According to this principle, some experts have suggested new types of structures for robots, including hip motion [40, 41], as shown in Fig. 5.

Fig. 5. Hip motion

One of the experiments on a new robotic platform that focuses on the mechanical structure and control of the hip joint has been carried out in [42]. The hip and basin oscillations allow for a larger step to smooth the CoM trajectory. The mechanism is divided into a universal joint actuated by parallel and a pin joint actuated by a link. The degrees of freedom of the yaw and roll are actuated cooperatively by a pair of parallel series elastic linear actuators to provide high joint torque and low leg inertia. The configuration of the hip joint actuator is shown in Fig. 6.

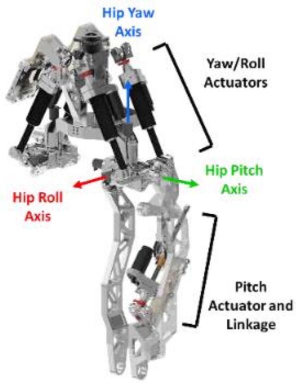

Fig. 6. Hip joint actuator configuration

8. *Arm swing*

The robot maintains a waist-moving torso without a rotating motion along a given trajectory and swings the arms back and forth around the shoulders in a specific plane. In a walking state, the robot naturally stretches its arms while lifting the forearms while running [40, 43-45]. It is expected to help reduce foot support contact and global walking costs. The arm swing modeling [40] is shown in Fig. 7.

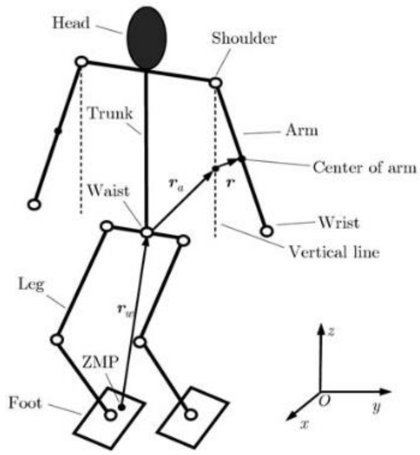

(a). Motion vectors representation of the arms swinging

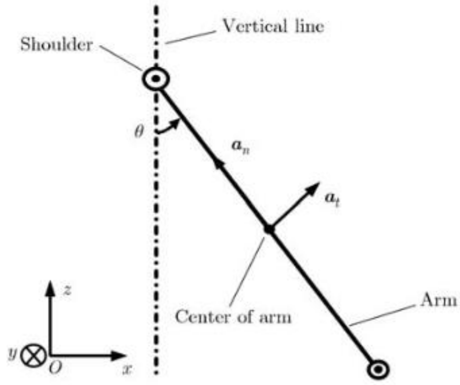

(b). Model illustration of arm swinging

Fig. 7. The arm swing modeling

B. Methods

In this study using a research methodology as shown in Fig. 8, with a brief explanation as follows.

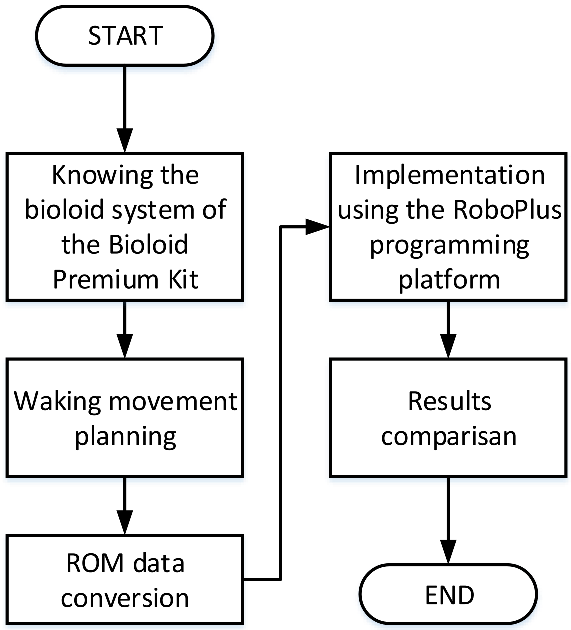

Fig. 8. research methodology

1. Bioloid System

The Bioloid System is an educational robot kit in a modular form that can help users to learn how a robot works. The robot kit is manufactured by ROBOTIS. Each set of Bioloid premium kits has a CM-530 robot controller, Dynamixel AX-12A servo, body parts, installer software, and various other supporting accessories.

In this study, A-type bioloid robot is used, with the object of study being the leg, as shown in Fig. 9, while the structure as shown in Fig. 10. The number of degrees of Freedom (DoF) on the robot's legs to the hip is 12 servos.

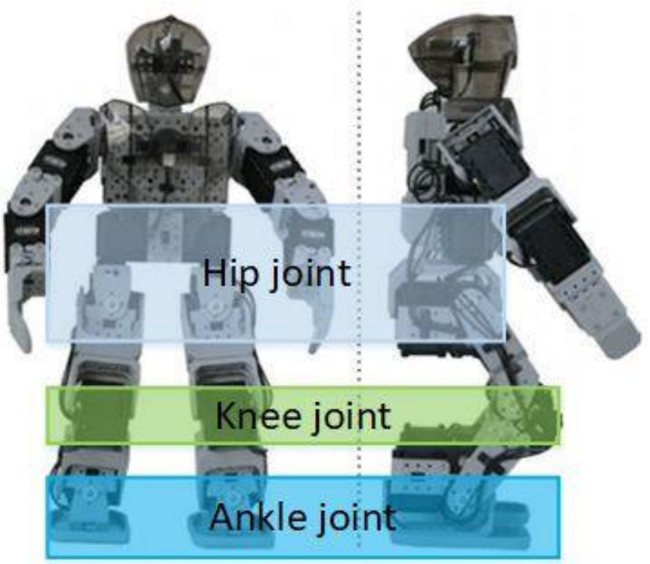

Fig. 9. The A-type bioloid robot's leg

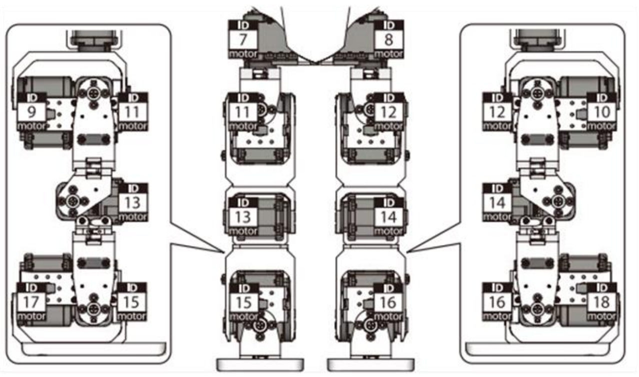

Fig. 10. The robot's leg stucture

A Dynamixel AX-12A servo-type actuator, as shown in Fig. 11, drives a bioloid robot's leg. This servo can detect speed, temperature, position, voltage and even protect itself, detecting errors that occur during the operation process. The range of movement of the Dynamixel AX-12A Servo is between $0^o - 300^o$ in degrees or 0 - 1023 in decimal units as shown in Fig. 11(b).

(a). physical form

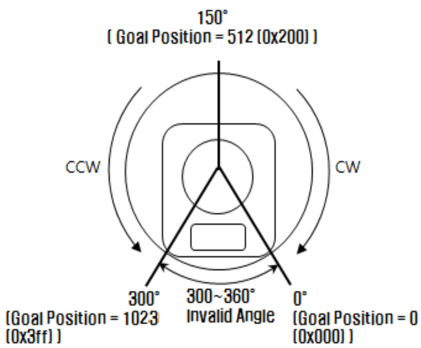

(b). AX series goal position

Fig. 11. Dynamixel AX-12A servo-type actuator

The servo angle value is calculated using the following formula:

$$\theta = (n^o / x^o) = y \ \ or \ \ \theta = (n/x)\, y^o \qquad (1)$$

where:

n^o	The value of the angle in degrees
x^o	The maximum value constant for the angular movement of the servo in degrees is (300^o)
y^o	The constant value for the maximum angular movement of the servo in decimal units (1023)
n	The value of the angle in decimal unit
x	The constant value for the maximum movement of the servo in decimal units (1023)
y	The maximum value constant for the angular movement of the servo in degrees is (300^o)

In this study, the A-type bioloid robot's leg is operated using a programmable CM530 controller, as shown in Fig. 12. This controller includes a CPU, TTL communication board, status LED, button input, and GP I / O port compatible with Dynamixel AX and MX series servo. This type of controller also supports network communications such as Bluetooth and ZigBee, which can also be connected to a PC via a USB port.

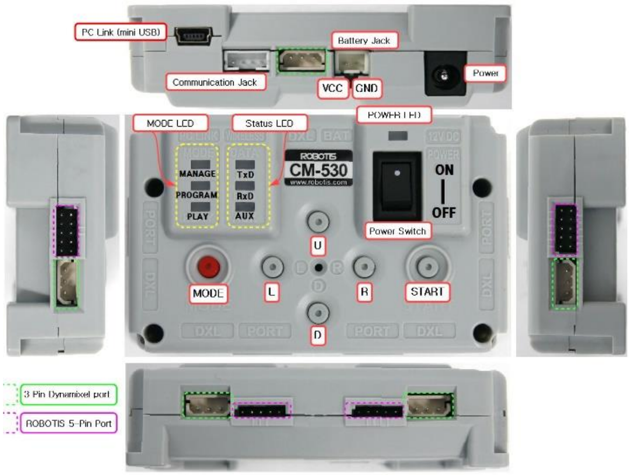

Fig. 12. CM 530 (Layout)

The CM 530 controller is operated using RoboPlus software (Fig. 13) made by ROBOTIS based on C-programming and consists of three main software utilities: (a). RoboPlus Task, (b). RoboPlus Manager, (c). RoboPlus Motion. In this study only use RoboPlus Manager and RoboPlus Motion. RoboPlus Manager manages controller firmware, checks the status of controllers and enhancements, and sets the necessary modes. Apart from that, Roboplus Manager is also used to set the ID and angle start position on the servo.

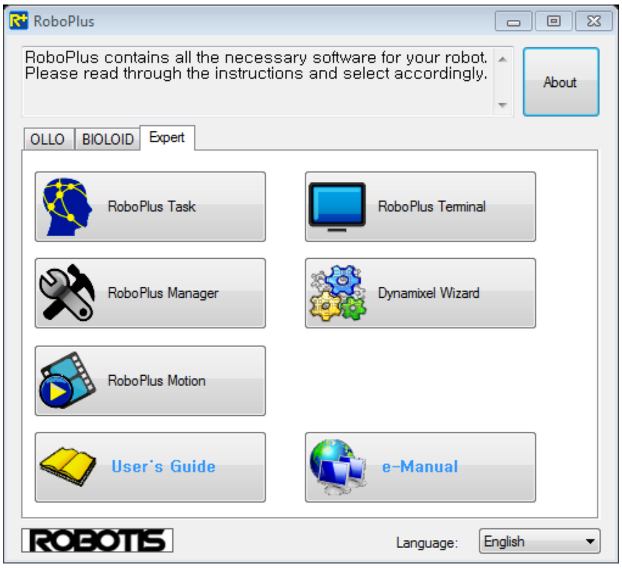

Fig. 13. RoboPlus

Following the robot structure, by default, some servo has a starting position, not at an angle of 512. Therefore, it is essential to determine the angular starting position on the servo to avoid the wrong initial movement position between one servo and another. The Roboplus Motion feature is used to create incremental movements based on rotation of the servo from the initial value to the final value.

The final controller that will be used in this study is OpenCM 9.04. It is a microcontroller board based on the 32bit ARM Cortex-M3. OpenCM 9.04 has 3 types, namely OpenCM 9.04-A, OpenCM 9.04-B, and OpenCM 9.04-C. This study using OpenCM 9.04-A, as shown in Fig. 14. OpenCM 9.04 can be programmed using the OpenCM IDE program. This program is open-source with various libraries and an example feature as a basic example for programming OpenCM 9.04, which can be modified easily.

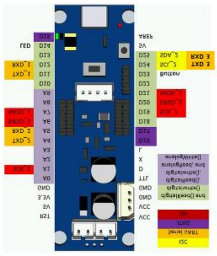

Fig. 14. OpenCM 9.04 type-A

Implementing human movement in robots requires Range of Motion (ROM) data on the human leg. ROM is a measurement of movement around a specific joint or body part. ROM data is used to determine how large the degree range of movement of the human joint is as a parameter of servo movement in the robot. ROM data is first converted using the following formula:

$$\theta = \left(\frac{n^o}{x^o}\right)\mathrm{y} + \mathrm{z} \quad or \quad \theta = \left(\frac{n^o}{x^o}\right)\mathrm{y} - \mathrm{z} \tag{2}$$

where:

n^o	ROM data on the human leg in degrees
x^o	the maximum value constant for the angular movement of the servo in degrees is (300^o)
y	The constant value for the maximum angular movement of the servo in decimal units (1023)
z	The constant value of the angle's default position on the servo in decimal units(512)
$y + z$	if the servo movement is clockwise (CW)
$y - z$	if the servo movement is counter-clockwise (CCW)

In this study, the basic movements planned are based on several types of traditional dances in Indonesia. The basic movements labelled with the motion number are as follows:

- *Motion* 1.
  The starting position of the robot, which is sitting.
- *Motion* 2.
  The robot is in the default position not standing upright, but with a slightly bent knee position.
- *Motion* 3.
  The robot tilts to the right to rest on the right leg before making the next movement.
- *Motion* 4.
  Robot raises left leg.
- *Motion* 5.
  The left leg moves forward with the ankle tilted slightly to the left to make it easier for the leg to move forward.

- *Motion* 6.
  The right and left legs move upright with the ankles.
- *Motion* 7.
  The right and left legs move, tilt to the left and rest on the left leg.
- *Motion* 8.
  Without moving the position of the left and right legs, the robot changes the forward leaning position by relying on the servo on the knee and the servo on the front ankle to maintain balance before making the next movement.
- *Motion* 9.
  Robot raises right leg.
- *Motion* 10.
  The right leg moves forward with the ankle tilted slightly to the right to make it easier for the leg to move forward.
- *Motion* 11.
  The right leg moves forward beyond the left leg.
- *Motion* 12.
  The right and left legs move upright with the ankles.
- *Motion* 13.
  The robot leans forward to support it before making the next move.
- *Motion* 14.
  Robot raises left leg.
- *Motion* 15.
  Left leg forward parallel to right leg.

The planned walking motion is then described into an algorithm, as shown in Fig. 15 are to be implemented into the RoboPlus programming platform.

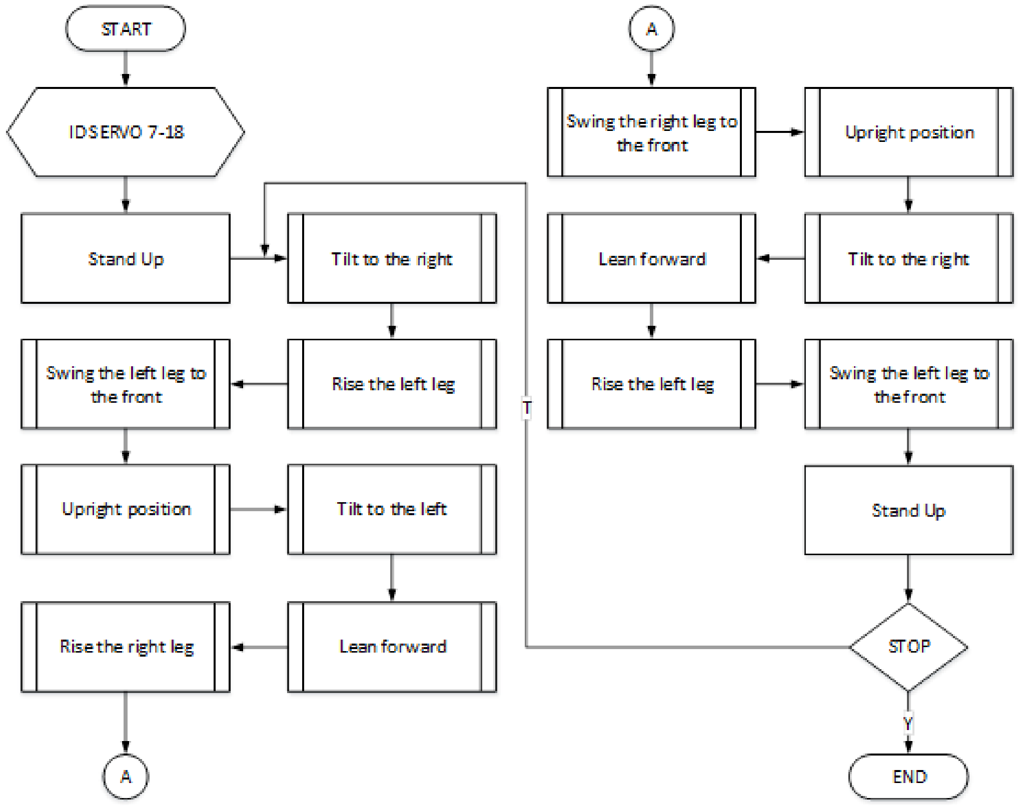

Fig. 15. The Walking Movement algorithm

III. Results and Discussions

A. Converting ROM data of the human leg to the robot leg

The list of movements that exist in the human leg for retrieval of ROM data was shown in TABLE I. The conversion of the movements for each part (hip, ankle, and knee) is done using Eq. (2). An example for the conversion of hip extension movements is as follows:

$$\theta_{right\ leg} = \left(\frac{30^\circ}{300^\circ}\right)1023 + 512 = 614.3$$
$$\theta_{left\ leg} = \left(\frac{30^\circ}{300^\circ}\right)1023 - 512 = -409.7 \quad (3)$$

The conversion result is shown in TABLE II. TABLE III. and 0

TABLE I. LEG MOTION

Motion	Hip	Ankle	Knee
Extension	1	X	1
Flexion	1	X	1
Abduction	1	X	X
Adduction	1	X	X
INT. Rotation	1	X	X
EXT. Rotation	1	X	X
Eversion	X	1	X
Inversion	X	1	X
Dorsiflexion	X	1	X
Plantarflexion	X	1	X

TABLE II. HIP ROM CONVERSION

Motion	ROM	without a default position value	with a default position value	
			Right leg	Left leg
Extension	30	102.3	614.3	409.7
Flexion	100	341	171	853
Abduction	40	136.4	375.6	375.6
Adduction	20	68.2	580.2	580.2
INT. Rotation	40	136.4	375.6	375.6
EXT. Rotation	50	170.5	682.5	682.5

TABLE III. ANKLE ROM CONVERSION

Motion	ROM	without a default position value	with a default position value	
			Right leg	Left leg
Extension	20	68.2	580.2	443.8
Flexion	40	136.4	648.4	375.6
Eversion	20	68.2	443.8	443.8
Inversion	30	102.3	614.3	614.3

TABLE IV. KNEE ROM CONVERSION

Motion	ROM	without a default position value	with a default position value	
			Right leg	Left leg
Extension	0	0	0	0
Flexion	150	511.5	1024	0.5

The entire conversion result is then used to provide a value for each servo ID in the hip, ankle and knee as shown in TABLE V. TABLE VI. TABLE VII. and TABLE VIII.

TABLE V. DEFAULT POSITION

NO.	SERVO ID											
1	7	8	9	10	11	12	13	14	15	16	17	18
	358	659	507	516	341	682	240	783	647	376	507	516
				This position is the starting position when later you will do a movement with your knees slightly bent.								

TABLE VI. HIP ROM

NO.	SERVO ID											
1	7	8	9	10	11	12	13	14	15	16	17	18
	358	659	512	512	512	614	512	512	512	512	512	512
	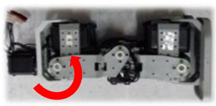			Extension movement cannot be done because of the limited motion of the robot structure								
2	7	8	9	10	11	12	13	14	15	16	17	18
	358	659	512	512	171	512	77	512	512	512	512	512
	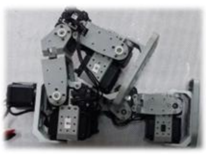			Flexion Movement. The next step is bending the knees								
3	7	8	9	10	11	12	13	14	15	16	17	18
	358	659	375	512	512	512	512	512	512	512	512	512
				Abduction. By positioning the right hip tilted to the right								
4	7	8	9	10	11	12	13	14	15	16	17	18
	358	659	580	575	512	512	512	512	512	512	512	512

				Adduction. By positioning the right hip tilted to the left. The position of the left hip also needs to be moved to facilitate movement of the right hip								
5	7	8	9	10	11	12	13	14	15	16	17	18
	358	659	375	512	211	512	203	512	512	512	512	512
				Internal Rotation. By positioning the right hip tilted outwards (right)								
6	7	8	9	10	11	12	13	14	15	16	17	18
	358	659	682	512	211	512	203	512	512	512	512	512
				External Rotation. By positioning the right hip tilted inward								

TABLE VII. ANKLE ROM

NO.	**SERVO ID**											
1	7	8	9	10	11	12	13	14	15	16	17	18
	358	659	512	512	211	512	203	512	580	512	512	512
	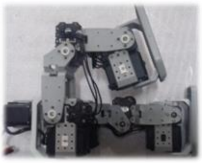			Extension. By bending, ankle up. The tip of the sole of the foot moves closer to the shin								
2	7	8	9	10	11	12	13	14	15	16	17	18
	358	659	512	512	211	512	203	512	580	512	648	512
	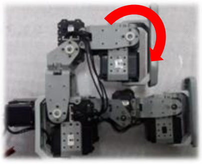			Flexion movement cannot be done because of the limited motion of the robot structure. The top of the foot moves away from the shin from the default position								
3	7	8	9	10	11	12	13	14	15	16	17	18
	358	659	512	512	211	512	203	512	512	512	443	512
				Inversion. By bending the right ankle oblique inward (left)								
4	7	8	9	10	11	12	13	14	15	16	17	18
	358	659	512	512	211	512	203	512	512	512	614	512
				Eversion. By bending the right ankle oblique outward (right)								

TABLE VIII. KNEE ROM

NO.	SERVO ID											
1	7	8	9	10	11	12	13	14	15	16	17	18
	358	659	512	358	659	512	512	512	512	512	512	512
				Extension movement. Knees, stay in an upright position because the knee remains 0°, where the default 512 on the robot leg is equal to 0° on the human leg								
2	7	8	9	10	11	12	13	14	15	16	17	18
	358	659	512	512	219	512	48	512	680	512	512	512
	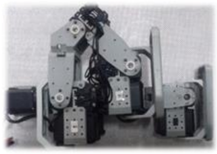			Flexion. By bending your knee by 150°								

B. *Implementation*

After converting ROM data in the previous stage, the next step is implementing it on the robot. Because the movement of the robot's legs is implemented from human movement, it is expected that the size of the servo movement when the robot is walking, which will later be made, will not exceed the existing range of movements. The results of the implementation are shown in TABLE IX. Red values correspond to ROM, and vice versa. The value 512 is the default position. The comparison results between the ROM value ranges and the value ranges obtained from the implementation are shown in TABLE X.

TABLE IX. THE WALKING MOVEMENT IMPLEMENTATION

ID	MOTION														
	1	2	3	4	5	6	7	8	9	10	11	12	13	14	15
7	358	358	358	358	358	358	358	358	358	358	358	358	358	358	358
8	669	669	669	669	669	669	669	669	669	669	669	669	669	669	669
9	515	507	555	555	555	507	469	466	516	520	507	507	560	531	535
10	515	516	551	551	550	516	474	473	514	515	516	516	553	523	523
11	307	341	340	340	340	340	340	428	404	366	347	347	337	336	336
12	736	682	682	769	711	711	711	682	682	682	682	682	624	686	685
13	54	240	239	239	239	239	239	236	270	231	298	298	227	225	225
14	970	783	782	818	728	728	728	783	783	783	783	783	784	814	772
15	749	647	647	647	647	647	647	720	706	676	567	567	640	640	640
16	291	376	375	446	460	460	460	376	376	376	376	376	324	364	427
17	513	507	558	558	558	507	466	475	469	458	494	507	558	558	558
18	504	516	552	549	555	516	469	472	472	472	472	516	549	548	546

TABLE X. THE COMPARISON RESULTS BETWEEN THE ROM VALUE RANGES AND THEIR IMPLEMENTATIONS

SERVO ID	ROM values range		From implementation	
	max	min	max	min
15	580	512	749	567
16	512	443	460	291

TABLE XI. PERFORMANCE RESULTS BASED ON THE DIFFERENCE IN VALUES

SERVO ID	Difference in value		% Error	
	max	min	max	min
15	169	55	29.14	10.74
16	52	152	10.16	34.31
	% Average error performance			21.09

IV. CONCLUSION

The conclusion that can be made from the study that has been carried out is that the movement program made can be implemented as expected. With some limitations where not all parameters that have been made can be implemented with a percentage of the success rate of 78.91%. For the further study to optimize the other functions of the servo, add the upper body to the ideal humanoid robot structure, and combine with other parameters for better results.

ACKNOWLEDGMENT

The authors would like to express their heartfelt thanks to all personnel of the Applied Modern Computing and Robotics System Unit, Politeknik Negeri Samarinda.

CONFLICT OF INTEREST

The authors declare no conflict of interest

REFERENCES

[1] PusPresNas, "Petunjuk Pelaksanaan Kontes Robot Indonesia (KRI) Tahun 2021," B. Kusumoputro, M. H. Purnomo, E. Mozef, H. S. BR, and G. Prabowo, Eds., ed. Jakarta: Kementerian Pendidikan dan Kebudayaan Republik Indonesia, 2021, https://kontesrobotindonesia.id/data/2021/.

[2] L. Vianello, L. Penco, W. Gomes, Y. You, S. Maria, Anzalone, P. Maurice, V. Thomas, and S. Ivaldi, "Human-humanoid interaction and cooperation: a review," *Current Robotics Reports, hal-03413650,* vol. 2, pp. 441-454, 2021.

[3] V. Potkonjak, "Is Artificial Man Still Far Away: Anthropomimetic Robots Versus Robomimetic Humans," *Robotics,* vol. 9, p. 57, 2020, http://doi.org/10.3390/robotics9030057.

[4] K. Somisetti, K. Tripathi, and J. K. Verma, "Design, Implementation, and Controlling of a Humanoid Robot," *2020 International Conference on Computational Performance Evaluation (ComPE), Shillong, India,* pp. 831-836, 2020.

[5] O. Stasse and T. Flayols, "An Overview of Humanoid Robots Technologies," vol. 124, pp. 281-310, 2019, http://doi.org/10.1007/978-3-319-93870-7_13.

[6] C.-c. Wong, S.-R. Xiao, and H. Aoyama, "Natural Walking Trajectory Generator for Humanoid Robot Based on Three-Mass LIPFM," *IEEE Access,* vol. 8, pp. 228151-228162, 2020.

[7] K. Yamamoto, T. Kamioka, and T. Sugihara, "Survey on model-based biped motion control for humanoid robots," *Advanced Robotics,* vol. 34, pp. 1353-1369, 2020.

[8] C.-c. Wong, S.-R. Xiao, and H. Aoyama, "Natural Walking Trajectory Generator for Humanoid Robot Based on Three-Mass LIPFM," *IEEE Access,* vol. 8, pp. 228151-228162, 2020, http://doi.org/0.1109/ACCESS.2020.30461066.

[9] T. Sugihara and M. Morisawa, "A survey: dynamics of humanoid robots," *Advanced Robotics,* vol. 34, pp. 1338-1352, 2020, https://doi.org/10.1080/01691864.2020.1778524.

[10] Z. Zhang, L. Zhang, S. Xin, N. Xiao, and X. Wen, "Robust Walking for Humanoid Robot Based on Divergent Component of Motion," *Micromachines,* vol. 13, Jul 11 2022.

[11] A. Kalouguine, C. Chevallereau, S. Dalibard, and Y. Aousti, "Periodic walkingmotion of a Humanoid robot based on human data," *uCoMeS 2020 New Trends in Mechanism andMachine Science. EuCoMeS 2020. Mechanisms and Machine Science,* pp. 349-359 2020.

[12] Y. Liu, Q. Bi, X. Zang, and Y. Li, "Human-like Walking of a Biped Robot Actuated by Pneumatic Artificial Muscles and Springs," *2020 16th IEEE International Conference on Automation Science and Engineering (CASE),* pp. 1395-1400, 2020.

[13] S. Yagi, N. Ise, S. Yu, Y. Nakata, Y. Nakamura, and H. Ishiguro, "Perception of Emotional Gait-like Motion of Mobile Humanoid Robot Using Vertical Oscillation," *Companion of the 2020 ACM/IEEE International Conference on Human-Robot Interaction,* pp. 529-531, 2020.

[14] T. Mikolajczyk, E. Mikolajewska, H. F. N. Al-Shuka, T. Malinowski, A. Klodowski, D. Y. Pimenov, T. Paczkowski, F. Hu, K. Giasin, D. Mikolajewski, and M. Macko, "Recent Advances in Bipedal Walking Robots: Review of Gait, Drive, Sensors and Control Systems," *Sensors,* vol. 22, Jun. 2022.

[15] R. Bogue, "Humanoid robots from the past to the present," *Industrial Robot: the international journal of robotics research and application,* vol. 47, pp. 465-472, 2020.

[16] G. H. Z. Liu, M. Z. Q. Chen, and Y. Chen, "When joggers meet robots: the past, present, and future of research on humanoid robots," *Bio-Design and Manufacturing,* vol. 2, pp. 108-118, 2019, https://doi.org/10.1007/s42242-019-00038-7.

[17] J. Lee, W. Hong, and P. Hur, "Continuous Gait Phase Estimation Using LSTM for Robotic Transfemoral Prosthesis Across Walking Speeds>," *IEEE Transactions on Neural Systems and Rehabilitation Engineering,* vol. 29, pp. 1470-1477, 2021.

[18] R. Kolaghassi, M. K. Al-Hares, and K. Sirlantzis, "Systematic Review of Intelligent Algorithms in Gait Analysis and Prediction for Lower Limb Robotic Systems," *IEEE Access,* vol. 9, pp. 113788-113812, 2021.

[19] B. Su and E. M. Gutierrez-Farewik, "Gait Trajectory and Gait Phase Prediction Based on an LSTM Network," *Sensors,* vol. 20, Dec 12 2020, http://doi.org/10.3390/s20247127.

[20] W. Yu, D. Jain, A. Escontrela, P. Xu, E. Coumans, S. Ha, J. Tan, A. Iscen, and T. Zhang, "Visual-Locomotion: Learning to Walk on Complex Terrains with Vision," *5th Conference on Robot Learning (CoRL 2021), London, UK.,* pp. 1-12, 2021.

[21] M. Khadiv, A. Herzog, S. A. A. Moosavian, and L. Righetti, "Walking Control Based on Step Timing Adaptation," *IEEE Transactions on Robotics,* vol. 36, pp. 629-643, 2020.

[22] S. Wang, S. Piao, X. Leng, Z. He, X. Bai, and L. Huazhong, "Real-Time Footprint Planning and Model Predictive Control Based Method for Stable Biped Walking," *Comput Intell Neurosci,* vol. 2022, p. 4781747, 2022.

[23] Q. Luo, "Self-stabilization of 3D Walking of a Biped Robot," *Robotics [cs.RO]. École centrale de Nantes, 2020. English, HAL Id: tel-03178308,* 2020.

[24] C. Jing and J. Zheng, "Stable walking of biped robot based on center of mass trajectory control," *Open Physics,* vol. 18, pp. 328-337, 2020, http://doi.org/10.1515/phys-2020-0148.

[25] X. Shi, J. Gao, Y. Lu, D. Tian, and Y. Liu, "Simulation of Disturbance Recovery Based on MPC and Whole-Body Dynamics Control of Biped Walking," *Sensors,* vol. 20, May 24 2020, http://doi.org/10.3390/s20102971.

[26] N. Scianca, D. D. Simone, L. Lanari, and G. Oriolo, "MPC for Humanoid Gait Generation: Stability and Feasibility," *IEEE Transactions on Robotics,* pp. 1-18, 2019.

[27] J. R. Sanchez-Ibanez, C. J. Perez-Del-Pulgar, and A. Garcia-Cerezo, "Path Planning for Autonomous Mobile Robots: A Review," *Sensors,* vol. 21, Nov 26 2021.

[28] C. Liu, J. Gao, D. Tian, X. Zhang, H. Liu, and L. Meng, "A Disturbance Rejection Control Method Based on Deep Reinforcement Learning for a Biped Robot," *Applied Sciences,* vol. 11, p. 1587, 2021.

[29] Z. Sun, "An energy efficient gait for Humanoid Robots Walking on even and uneven terrains," Dissertation, Department of Data Science andKnowledge Engineering, Maastricht University, 2019, https://doi.org/10.26481/dis.20190327zs.

[30] H. Wu, W. Xu, B. Yao, Y. Hu, and H. Feng, "Interacting Multiple Model-Based Adaptive Trajectory Prediction for Anticipative Human Following of Mobile Industrial Robot," *24th International Conference on Knowledge-Based and Intelligent Information & Engineering Systems, Procedia Computer Science 176 (2020) 3692–3701,* vol. 176, pp. 3692-3701, 2020.

[31] I. Maroger, O. Stasse, and B. Watier, "Walking Human Trajectory Models and Their Application to Humanoid Robot Locomotion," *2020 IEEE/RSJ International Conference on Intelligent Robots and Systems (IROS),* pp. 3465-3472, 2020.

[32] D. Ahn and B.-K. Cho, "Optimal Standing Jump Trajectory Generation for Biped Robots," *International Journal of Precision Engineering and Manufacturing,* vol. 21, pp. 1459-1467, 2020, http://doi.org/10.1007/s12541-020-00360-6.

[33] F. Zhao and J. Gao, "Anti-Slip Gait Planning for a Humanoid Robot in Fast Walking," *Applied Sciences,* vol. 9, p. 2657, 2019.

[34] S. Savin, "ZMP-Based Trajectory Generation for Bipedal Robots Using Quadratic Programming," *Control and Signal Processing Applications for Mobile and Aerial Robotic Systems,* pp. 266-285, 2020.

[35] B. Park and J. Park, "Walking Pattern Generation using MPC with minimization of COM Velocity Fluctuation," *2020 20th International Conference on Control, Automation and Systems (ICCAS 2020),* pp. 268-273, 2020.

[36] Y. Lee, H. Lee, J. Lee, and J. Park, "Toward Reactive Walking: Control of Biped Robots Exploiting an Event-Based FSM," *IEEE TRANSACTIONS ON ROBOTICS,* pp. 1-16, 2021.

[37] A. Maiorino and G. G. Muscolo, "Biped Robots With Compliant Joints for Walking and Running Performance Growing," *Frontiers in Mechanical Engineering,* vol. 6, 2020. http://doi.org/10.3389/fmech.2020.00011.

[38] C. Liu, W. Geng, M. Liu, and Q. Chen, "Workspace Trajectory Generation Method for Humanoid Adaptive Walking With

Dynamic Motion Primitives," *IEEE Access*, vol. 8, pp. 54652-54662, 2020.

[39] O. Drama and A. Badri-Sprowitz, "Trunk pitch oscillations for energy trade-offs in bipedal running birds and robots," *Bioinspir Biomim*, vol. 15, p. 036013, Mar. 2020.

[40] M. Ceccarelli, M. Russo, and C. Morales-Cruz, "Parallel Architectures for Humanoid Robots," *Robotics*, vol. 9, p. 75, 2020.

[41] G. Ficht and S. Behnke, "Bipedal Humanoid Hardware Design: A Technology Review," *Current Robotics Reports, Springer*, vol. 2, pp. 201-210, 2021.

[42] H. El Daou, K. C. G. Ng, R. Van Arkel, J. R. T. Jeffers, and Y. B. F. Rodriguez, "Robotic hip joint testing: Development and experimental protocols," *Med Eng Phys*, vol. 63, pp. 57-62, Jan 2019, http://doi.org/10.1016/j.medengphy.2018.10.006.

[43] F. L. Haufe, A. M. Kober, P. Wolf, R. Riener, and M. Xiloyannis, "Learning to walk with a wearable robot in 880 simple steps: a pilot study on motor adaptation," *J Neuroeng Rehabil*, vol. 18, p. 157, Nov 1 2021.

[44] H. Mineshita, T. Otani, M. Sakaguchi, Y. Kawakami, H. O. Lim, and A. Takanishi, "Jumping Motion Generation for Humanoid Robot Using Arm Swing Effectively and Changing in Foot Contact Status," *2020 IEEE/RSJ International Conference on Intelligent Robots and Systems (IROS)*, pp. 3823-3828, 2020.

[45] A. Miyata, S. Miyahara, and D. N. Nenchev, "Walking With Arm Swinging and Pelvis Rotation Generated With the Relative Angular Acceleration," *IEEE Robotics and Automation Letters*, vol. 5, pp. 151-158, 2019, DOI: 10.1109/LRA.2019.2948529.